Interface of Covalently Bonded Phospholipids with a Phosphorylcholine Head: Characterization, Protein Nonadsorption, and Further Functionalization

Lynda Ferez, Thierry Thami, Edefia Akpalo, Valérie Flaud, Lara Tauk, Jean-Marc Janot, Philippe Déjardin

Interface of Covalently bonded phospholipids with a phosphorylcholine head: characterization, protein non adsorption and further functionalization

Lynda Ferez[a], *Thierry Thami*[a], *Edefia Akpalo*[a], *Valérie Flaud*[b], *Lara Tauk*[a], *Jean-Marc Janot*[a], *Philippe Déjardin*[a]*

[a] Institut Européen des Membranes, Université Montpellier 2 (ENSCM, UM2, CNRS), CC047, 2 Place Eugène Bataillon, F-34095 Montpellier Cedex 5 (France)

[b] XPS Technological platform, Institut Charles Gerhardt, Université Montpellier 2, 2 Place Eugène Bataillon, F-34095 Montpellier Cedex 5 (France)

philippe.dejardin@iemm.univ-montp2.fr,

Running title: PMHS-phosphorylcholine

*Corresponding author, philippe.dejardin@iemm.univ-montp2.fr, Tel +33467149121, Fax +33467149119. Part of the paper was presented at Nanomedicine-2010 Congress, Beijing (China), Oct. 23-25, 2010.

ABSTRACT Surface anchored poly(methylhydrosiloxane) (PMHS) thin films on oxidized silicon wafers or glass substrates were functionalized via the SiH hydrosilylation reaction with the internal double bonds of 1,2-dilinoleoyl-sn-glycero-3-phosphorylcholine (18:2 Cis). The surface was characterized by X-ray photoelectron spectroscopy, contact angle measurements, atomic force microscopy and scanning electron microscopy. These studies showed that the PMHS top layer could be efficiently modified resulting in an interfacial high density of phospholipids. Grafted phospholipids made the initially hydrophobic surface ($\theta = 106°$) very hydrophilic and repellent towards avidin, bovine serum albumin, bovine fibrinogen, lysozyme and α-chymotrypsin adsorption in phosphate saline buffer pH 7.4. The surface may constitute a new background-stable support with increased biocompatibility. Further possibilities of functionalization on the surface remain available owing to the formation of interfacial SiOH groups by Karstedt-catalyzed side reactions of SiH groups with water. The presence of interfacial SiOH groups was shown by zeta potential measurements. The reactivity and surface density of SiOH groups were checked by fluorescence after reaction of a monoethoxy silane coupling agent bearing alexa as fluorescent probe.

Keywords: biocompatibility; phosphorylcholine; biosensor; PMHS; silicone gel; hydrosilylation; phospholipid; antifouling

Introduction

The efficiency of sensors for biomedical analysis is dependent on the integrity and accessibility of the surface-fixed molecule designed for molecular recognition, on the one hand, and on the surroundings designed for neutral behavior, especially to avoid non specific adsorption, on the other hand. The last requirement leads in practice to diagnostic kits using blocking buffers containing typically albumin[1, 2]. Neutral behavior is also required for biomaterials where the biological functions of the fluid components have to be preserved. For instance, the proteins should present no conformational changes in solution,

possibly induced by adsorption at interfaces, as this could trigger cascades of biological reactions.[3] Even active biomaterials for cell culture, for instance, could be considered as surfaces with specific anchoring and functional points positioned on a neutral surface.

Several strategies were considered to create surfaces with neutral behavior. They can be roughly classified into two categories:[4] the first being based on poly(ethylene oxide) –PEO –,[3, 5-16] and the second on zwitterionic groups[17-19], especially the phosphorylcholine head. The reason for their efficiency is that they are very hydrophilic. They can retain numerous molecules of water. The choice of a phosphorylcholine (PC) head is justified by the large number of phospholipids bearing that head on the external side of the bilayer membrane of cells.[20] Phospholipid polymers were developed many years ago.[21-26] Chemical transformation of the phospholipids was then necessary to obtain first the polymerizable functional group as was the case when individual surface grafting was carried out.[27] The availability of 2-methacryloyloxyethyl phosphorylcholine (MPC) monomer has resulted in several studies with polymers based on this monomer [28-37] in particular recently when the reaction of the monomer with triethoxysilane was investigated before covalent fixation on titanium alloy[38]. Modification of existing polymers to obtain PC side chains was carried out for polyelectrolyte multilayer applications.[39] Grafting of PC on hydroxylated gold surfaces was also studied.[40] Instead of considering synthesis and adsorption of various (co)polymers containing PC or ethylene oxide (EO) chains, we looked at the possibility of creating soft structures aimed at covalent bonding of these groups in high density. In the present study PC grafting was considered preferable to EO where hydration layer stability decreases as the temperature increases.[41] Moreover, polymers based on EO can decompose in the presence of oxygen and transition metal ions.[42]

We followed the strategy of hydrosilylation. Silicone gels such as polydimethylsiloxane (PDMS) have been previously considered as starting materials requiring surface modification to improve biocompatibity. The aim was to introduce Si-H functional groups for subsequent reactions. Several approaches have been developed to introduce SiH onto silicone gels such as plasma treatment,[43] acid catalyzed equilibration in the presence of polymethylhydrosiloxane (PMHS),[44, 45] and

copolymerization.[46-48] Indeed, hydrosilylation of an alkene C=C by addition of SiH is a very effective reaction in the bulk or in solution by using platinum catalysts.[49-51] The reaction is irreversible and the resulting Si-C bond is hydrolytically stable. In addition PMHS gels have been shown to be stable for several months[52, 53] before subsequent functionalization. The functional SiH groups are used to add hydrophilic moieties like PEO [44-48] or PC groups *via* the monomer MPC[54] thus increasing the protein repellent properties. These methods often result in incomplete surface coverage after hydrosilylation with the functional molecule, partly due to a low density of SiH groups.

We developed recently a new method that allows control of the accessibility of SiH groups by using sol–gel process of lightly crosslinked PMHS materials in order to increase the functionalization density of silicone layers by the molecule of interest[55, 56]. The sol-gel process allowed a facile and rapid formation of a thin PMHS layer covalently grafted on the silica surface at room temperature. In addition, the process of film crosslinking and surface attachment on silica occurs in one step giving homogeneous and flat films in the nanometer range allowing further reaction with alkenes[56]. PMHS layers were prepared by acid-catalyzed hydrolytic polycondensation of a mixture of methyldiethoxysilane monomer and triethoxysilane as crosslinker. Moreover, it was shown that in a soft network (5% of crosslinker) complete platinum catalyzed addition of alkene molecules up to C_{18} could occur[55]. We believe that this method has opened a new way to obtain very hydrophilic domains with high density of moieties like EO or PC.

The present work was therefore focussed on the functionalization of oxidized silicon wafers and glass substrates with PC via PMHS. Instead of synthesizing molecules with the PC functional group, we took advantage of the availability of phospholipids with long fatty chains which would also give a closer biomimetism of the cell bilayer membrane surface. The large molecular size should moreover lead to only limited functionalization inside the bulk of the layer but quantitative functionalization at the surface of the material. Contrary to the material obtained from photopolymerization of diacetylenic phospholipids,[25] the final layer should not be colored. Moreover additional stabilizing hydrophobic interactions between the fatty chains are expected in an aqueous environment. Such stabilization of the

assembly of non covalently bonded phospholipids has also been achieved by heating / cooling.[57] Previously[58] other studies concluded that for polymerized planar supported bilayers, to ensure quantitative lipid retention upon removal from water, all the lipids must be covalently anchored to the polymer network. Also important is the absence of defects.[59] The high density of SiH functional groups could also favor complete consumption of the unsaturated carbon-carbon bonds leading to a final product protected against self-oxidation. In summary we adopted the strategy, which we have previously applied in the development of a sensor for nitroaromatics[60], of establishing first a soft thin three-dimensional network scaffold where unsaturated phospholipids could be subsequently grafted in a second step.

With this aim, we first deposited by the sol-gel process an anchored layer of the PMHS network and functionalized it afterwards by reaction of the silane groups with the unsaturated phospholipid 1,2-dilinoleoyl-sn-glycero-3-phosphorylcholine (18:2 Cis). The commercially available phospholipid molecule bearing four unsaturated double bonds which are all reactive toward hydrosilylation was chosen in order to be able to observe a significant infrared absorption signal of the C=C bond for the bulk starting material. A 1 μm thick PMHS layer allowed this common infrared analysis. The final product interface was characterized by photoelectron spectroscopy (XPS), captive bubble contact angle measurements in water, atomic force microscopy (AFM) and scanning electron microscopy (SEM). The adsorption of avidin, bovine serum albumin, bovine fibrinogen, lysozyme and α-chymotrypsin were studied by means of normal scanning confocal fluorescence. We used a method for the quantitative determination of interfacial concentration. In addition, creation of new functional groups at such interfaces was shown to be easy and their interfacial density was determined by the same method.

Materials and Methods

Chemicals

Both precursors methyldiethoxysilane $HSi(CH_3)(OCH_2CH_3)_2$ (DH) and triethoxysilane $HSi(OCH_2CH_3)_3$ (TH) were purchased from ABCR (Karlsruhe, Germany) and used as received. Water for substrate cleaning was obtained from a Milli-Q water purification apparatus (Millipore). Absolute ethanol for sol−gel synthesis was of synthesis grade purity. The sol-gel catalyst trifluoromethanesulfonic acid CF_3SO_3H was purchased from Aldrich. Toluene for thin film hydrosilylation was distilled before use. The platinum-divinyltetramethyldisiloxane complex in xylene (platinum concentration *ca.* 0.1 M assuming 2.4% (w) Pt in xylene), also known as Karstedt's catalyst, was purchased from ABCR (PC072). 1,2-dilinoleoyl-sn-glycero-3-phosphorylcholine (18:2 Cis) (PL, Fig. 1) was purchased from AvantiPolarLipids.

Other chemicals were used as received: 3-(ethoxydimethylsilyl)-propyl amine (Aldrich, 588857), Alexa Fluor® 594 succinimidyl ester (labelling kit A10239, InvitroGen), biotin-ethylenediamine hydrobromide (Sigma B9181).

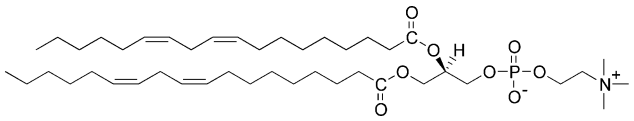

Figure 1 Structure of 1,2-dilinoleoyl-sn-glycero-3-phosphorylcholine (18:2 Cis).

Proteins and labeling

Bovine serum albumin (A-7638), bovine fibrinogen (F-8630), lysozyme (62971-Fluka), α-chymotrypsin (C-4129) and avidin (A9275) were purchased from Sigma-Aldrich; some avidin from Fluka (No. 11368). Labeling of proteins was performed with Alexa-fluor-594 succinimidyl ester (InvitroGen, A30008). Typically 500 µL of protein solution were added to dry fluorophore Alexa-594 in molar ratio 1:1 and allowed to react for 0.5 h at 20°C. Avidin was also labelled *via* the previous biotin-ethylenediamine hydrobromide reaction with alexa succinimidyl ester as described elsewhere [61]. The mixture was then put in an *ad hoc* microtube with filter (Biospin P6) and centrifuged at 16 000 g for 1 min according to the supplier of the kit. The labeling ratio [Alexa] / [protein] (0.3-0.5) was determined

from the UV absorbances at 280 nm where both the label ($\varepsilon_{280\,-Alexa}$ = 50 400 M^{-1} cm^{-1}) and the protein absorb and at 590 nm where only the label (ε_{590} = 90 000 M^{-1} cm^{-1})[62] absorbs. Protein solutions were prepared in 10mM sodium phosphate buffer pH 7.4 with 0.15M NaCl in de-ionized water (MilliQ system, Millipore) and stored at 4°C.

Substrate cleaning and activation

Silicon wafers Si(100) (ACM, France) cut into square strips of 2 × 2 cm^2 or thin microscope glass slides (see below) were used as substrates for spin-coating deposition. The square was cut into four pieces of 1 cm^2 area for phospholipid reaction with the PMHS layer. To bond covalently the PMHS thin films to native oxide silica (thickness ~ 2 nm), the silicon wafers were first cleaned and activated using the previously described procedure with "piranha" solution H_2SO_4/H_2O_2-30%w (70/30 vol); 90°C; 30 min.[53] *Caution: piranha solution must be handled extremely carefully*. For fluorescence adsorption measurements, the substrates were wafers or thin microscope glass slides (Menzel-Glazer, Germany) of 2.5 × 6 cm^2 submitted to the same treatment to bond PMHS. However, for protein adsorption to glass (without subsequent PMHS bonding), the substrate was previously treated with sulfochromic acid and rinsed carefully just before adsorption experiment.

PMHS films

PMHS thin films were prepared at 22 ± 1 °C by sol–gel polymerization of DH and TH as crosslinker. DH/TH 95/5 (mol%) sol mixtures were deposited by spin-coating on freshly activated substrates according to the procedure[55, 56] summarized as follows. Trifluoromethanesulfonic acid CF_3SO_3H (1.0 M in absolute ethanol) was used as catalyst (0.5 mmol/mol of monomers). The mixture of monomers (4.0 M in EtOH; molar ratio [EtOH]/[Si] = 1) was polymerized with hydrolysis ratio h = $[H_2O]/[SiOEt]$ = 0.5. The content of trifluoromethanesulfonic acid was not higher than 0.05% to control the kinetics of gelation of the liquid mixture. The resulting clear sols were allowed to age for ~30

minutes with magnetic stirring before spin-coating deposition. The freshly cleaned silicon wafer was purged (2 min) in the spin-coater (Spin150, SPS Europe) under a stream of nitrogen (2 L/min) to avoid air moisture. For all samples, the speed of rotation was 4000 rpm (spin acceleration 2000 rpm/s) and the rotation time 30 s. The samples were finally cured at 110°C in an oven for 15 minutes. This procedure gave layers of reproducible homogeneity and thickness as verified by electron microscopy and infrared analysis.

Grafting PMHS with phospholipid to afford PL-PMHS

After spin-coating a *ca.* 1µm thick PMHS layer onto pieces of oxidized silicon wafer, the hydrosilylation reaction between the dilinoleoyl phospholipid and the PMHS SiH functional group was performed in air by casting solutions of phospholipid in the presence of Karstedt's catalyst. The reaction was then allowed to proceed in air at two different temperatures, 20°C and 40°C, before the sample was rinsed to remove any physisorbed material, and finally dried under a stream of nitrogen.

The phospholipid solutions contained 20 mg in 1 mL of toluene (25.5 mM), with an additional 2µL of the xylene solution of the platinum divinyltetramethyldisiloxane complex. To functionalize the PMHS film (thickness ca. 1 µm or less, area 1 cm^2), droplets of the phospholipid solution were deposited on PMHS by casting. Typically, four coalescing droplets of 5 µL were enough to cover the PMHS area. The procedure was repeated over 15 -30 min until a final molar ratio of phospholipid in excess of 1.5 over the SiH groups present on the PMHS film was achieved. After total evaporation of the toluene (*ca.* 15 min) at room temperature, the samples were kept for 15h (A) at 20°C or (B) placed in a thermostated box at 40°C. The samples were then rinsed three times in 5 mL of dry toluene. To remove any non-covalently bonded molecules in both procedures A and B the samples were immersed successively in different toluene/chloroform mixtures ranging from 100% to 0% (vol.) toluene with in steps of 20%. The samples were dried under a stream of nitrogen for 5 minutes, then immersed in water for two hours and finally re-dried. Transmission infrared (IR) absorption spectra of the thin films before and after

hydrosilylation were used to ascertain the reaction yield after solvent and water rinsing. The water drop or air captive bubble contact angle in water was finally measured in order to characterize the sample surface hydrophilicity.

Synthesis of monoethoxysilane bearing Alexa. Grafting on PL-PMHS

To a solution of Alexa Fluor® 594 succinimidyl ester (12.2 nmol) in dry ethanol (100 µL) under an argon atmosphere, was added 3-(ethoxydimethylsilyl)-propyl amine (12.2 nmol). The reaction mixture was vigorously stirred for two hours at room temperature. The resulted mixture was then divided into ten parts. The solvent was evaporated under reduced pressure and the product alexa-monoethoxysilane thus obtained was used without further purification. HRMS (Q-Tof) : Calcd for $C_{35}H_{35}N_3O_{10}S_2$ 721.1745 (M^- - $C_4H_{11}SiO$); found: 721.1764.

PL-PMHS functionalization: Each part of the divided alexa-monoethoxysilane (~ 1 nmol) was dissolved in a mixture of toluene/dry ethanol (700µL/300µL). The PL-PMHS coated surfaces were then soaked in the solution for one hour. The substrates were further rinsed with ethanol, dried under a stream of argon, then kept overnight in Milli-Q water in order to remove any trace of physically adsorbed alexa before characterisation by confocal microscopy.

PL-PMHS passivation with hexamethyldisilazane (HMDS): The substrate with a PL-PMHS layer was dried under a stream of argon and treated with a solution of 95-5 % (vol.) of dry toluene-HMDS for 30 min at room temperature. After rinsing with toluene, and drying under a stream of argon, the substrate was soaked in alexa-monoethoxysilane solution as described above.

X-ray photoelectron spectroscopy (XPS)

The surface elemental composition of the PMHS and PL-PMHS surfaces were analysed by XPS. The spectra were obtained by means of a spectrophotometer (ESCALAB 250, Thermo Electron, UK) equipped with a monochromatic Al Kα (1486.6 eV) radiation source. The acceleration tension and power of the X-ray source were 15 kV and 100 W, respectively. The samples were analysed in the 10^{-9} mbar range of pressure. The photoelectrons were analyzed at normal incidence of the sample surface. The spot size was approximately 400μm^2. The composition corresponds to depths of 5-10 nm. Survey scans (0-1350 eV) at low resolution were performed to identify the constitutive elements. High resolution C_{1s}, Si_{2p}, O_{1s}, N_{1s} and P_{2p} spectra were recorded to obtain more detailed information on the nature of the surface. The peaks were fitted with Gauss–Lorentz curves. They provided the various surface atomic ratios which were calculated from the ratio of the corresponding peak areas, assuming the total area corresponded to 100%, after correction with the theoretical sensitivity factors reported by Scofield.[63] The spectra of both pristine PMHS and PL-PMHS were calibrated using the hydrocarbon contaminant or alkane C_{1s} peak at 284.8 eV. In both cases, the peak of Si-$\underline{C}H_3$ was found at a binding energy (BE) of 284.0 eV in agreement with PDMS polymer at 284.4 eV according to Beamson and Briggs.[64]

Captive air bubble contact angle measurements in water

Air captive bubble contact angles in water were measured (GBX - Digidrop, Romans, France) by applying an air bubble of about 25 µL to the surface. Contact angles with water were measured by applying a water droplet of 7 µL to the surface. The contact angle was calculated using computerized image analysis.

Adsorption: Determination of interfacial concentration

The experiments were performed at T = 19°C in a slit flow cell of thickness 63 or 105 µm and flow rate corresponding to wall shear rate 1000 s^{-1}. Confocal measurements were performed at 3 cm from the slit entrance. Details were provided in a previous work.[65] The entrance design was modified to provide a sharper transition between the flows of buffer and solution. The interfacial concentration was evaluated as follows: the fluorescence signal F_{sol} from the solution at concentration C is relative to an effective volume V while the signal F_{surf} at the surface concerns the interfacial concentration Γ over area A. $F_{surf} \propto \Gamma A$ and $F_{sol} \propto C V$ therefore $\Gamma = (V/A)\,(F_{surf}/F_{sol})\,C$. In a previous paper[66] the order of magnitude of V/A was estimated from the focus radius for A and 1 μm^3 taken as the confocal volume V. We propose below the experimental determination of V/A according to the following argument.

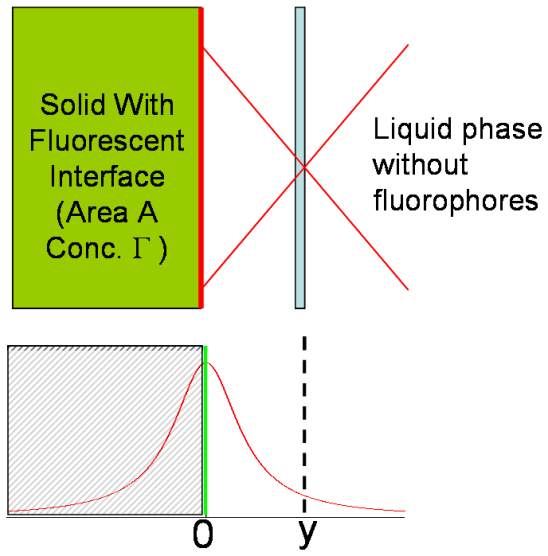

Figure 2 (top) Scheme of focused laser beam at some distance from an interface occupied by fluorescent molecules. No fluorescent molecules in solution. (bottom) Resulting peak $F_i(y)$ from normal scanning to the interface.

We consider the interfacial signal $F_i(y)$ obtained under the confocal mode by scanning normal to a fluorescent interface positioned at $y = 0$ in non fluorescent solution (Fig. 2). $F_i(y)$ is maximal at $y = 0$; $F_{surf} = F_i(0)$ When focusing at position $y \neq 0$, the emission signal which originates from fluorescent molecules at position y = 0 is smaller by some factor given by the normalized curve to its maximum $f_i(y)$

= $F_i(y)$ / $F_i(0)$. Assuming random orientation of the fluorophores, whatever the beam polarization and surface concentration, the signal is proportional to the number of molecules on the emitting area A where the concentration is Γ (mass or mol per unit area). $F_{surf} \propto \Gamma A$. Let us consider now focusing with the same beam into a solution of uniform concentration C_b (mass or mol per unit volume). $F_{sol} \propto C_b V$. In that situation the emission signal when focusing at some distance y_0 originates from the same area A excited at position y_0 and from other molecules in the neighborhood of y_0. The contribution to the signal at y_0 from a plane of thickness dy situated at distance Δy is $dF_{sol} \propto A\, dy\, C(y_0 + \Delta y)\, f_i(\Delta y)$. The observed signal is the sum of those elementary contributions. Assuming the concentration to be constant and the space infinite, we have:

$$F_{sol} \propto AC_b \int_{-\infty}^{+\infty} f_i(y)\, dy \qquad (1)$$

The integral is the area under the curve $f_i(y)$ and has the dimension of length. Let us call it w_D, subscript D reminding that its determination comes from the convolution of the laser beam with a fluorescent surface described as a Dirac function. Then the ratio V / A is the integral of the interfacial signal normalized to its maximum. $\Gamma = w_D\, (F_{surf} / F_{sol})\, C$. The product $w_D\, F_{surf}$ is anyway the area under the curve $F_i(y)$. The parameter w_D was determined from the signal of the interface after replacing the solution by buffer, since adsorption was either irreversible or very slow desorption occurred. Several functions can be used to fit the data. We found that a linear combination of Lorentzian and Gaussian functions provided a satisfactory fit. Three examples are given in Fig. 3. The width w_D was reproducible over one experiment and the variations were small from one experiment to another (relative variation of about 10%). The convolution of the solution profile (step function at both interfaces) with the beam shape leads to a sigmoid at the interfaces with half the bulk solution signal at the interface [66]. We used then as surface signal F_{surf} the raw signal minus half the solution signal. This correction was negligible when a strong adsorption occurred at small solution concentrations.

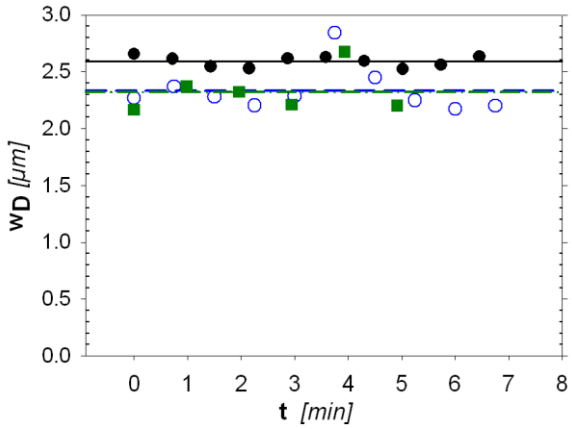

Figure 3 Peak width w_D at interface, determined from adsorbed avidin, as a function of time in the presence of the rinsing flowing buffer after flowing solution. (●) hydrophilic glass, w_D = 2.59 ± 0.01 (Std Error) µm; (o) Glass covered with 1 µm thick PMHS, w_D = 2.33 ± 0.06 µm; (■) Glass covered with phospholipid-functionalized PMHS, right after preparation, w_D = 2.32 ± 0.08 µm.

AFM and SEM

Atomic Force Microscopy (AFM) experiments were performed using a Dimension 3100 microscope equipped with a Nanoscope IIIa controller system (Digital Instruments, Veeco Metrology Group). AFM images were obtained by scanning in tapping mode in water or under air ambient conditions using silicon SPM probes (stiffness $k \approx 2$ N/m, resonance frequency of 67 kHz, pointeprobeplus, Nanosensors). The root mean square average roughness (R_q) was analyzed by the Nanoscope software (version 5.31r1). Scanning electron microscopy (SEM) pictures were obtained with a Hitachi S4800 instrument. The MeX software (version 5.1) was used for the construction of the 3D SEM image and z-profile (±10 nm) from differently tilted SEM images.

Results and Discussion

A previously-reported novel reactive polymethylhydrosiloxane polymer crosslinked by the sol-gel reaction of hydrogenosilane precursors was prepared allowing subsequent functionalization by hydrosilylation of the SiH groups[55, 56]. The hydrosilylation reaction between the internal double bonds of the phospholipid molecule and the PMHS SiH functional group occurred in air under very mild conditions at only 20°C or 40°C in the presence of the platinum catalyst.

Chemical analysis of the Interfaces

The XPS composition of the pristine PMHS surface showed good agreement with the theoretical elemental composition (hydrogen excluded) of the bulk PMHS-network $(SiCO_{2/2})_{0.95}(SiO_{3/2})_{0.05}$. However the ratio *C/Si* (0.80) was lower than the theoretical value (0.95). The content of methylhydrogenosiloxane difunctional subunits $SiHCH_3O_{2/2}$ was then lower than expected probably due to partial evaporation of DH oligomers.[53] After hydrosilylation of PMHS with PL, the infrared sharp absorption C=C peak at 3009 cm^{-1} of the cis-double bond in the starting PL spectrum totally disappeared in the final PL-PMHS film. This suggested complete reaction has occurred of the unsaturated carbon-carbon bonds of phospholipids. Nitrogen (N_{1s}) and phosphorus (P_{2p}) peaks, attributed to the ammonium $N^+(CH_3)$ and phosphate PO_4^- groups of the phosphorylcholine subunit[31,32,33] appeared at 402.7 and 133.5 eV, respectively. The *O* content was higher than expected because the SiH group in PMHS matrix underwent reaction with water (present from air moisture) catalyzed by Karstedt's catalyst.[56] However, it was not easy by XPS to differentiate the SiOH and SiOSi groups. The elemental surface composition can be thus calculated with the following structure without hydrogen and neglecting the TH crosslinker: $[(C_{44}NO_8P)_{1/4}(SiCO_{2/2})]_z\ [SiCO_{3/2}]_{1-z}$ where *z* is the fraction of SiH having reacted with the double bonds of PL; the complement 1-*z* having reacted with water to form SiOH and new Si-O-Si links. Experimental atomic percentages agree well with $z \approx 0.45$. The presence of superficial SiOH was sustained by streaming potential measurements (Fig. 4) in the presence of 10^{-3} M KCl. The negative ζ

potential (-65 mV) cannot be explained by the phosphorylcholine head and the isoelectric point is clearly in the acidic domain of silica.

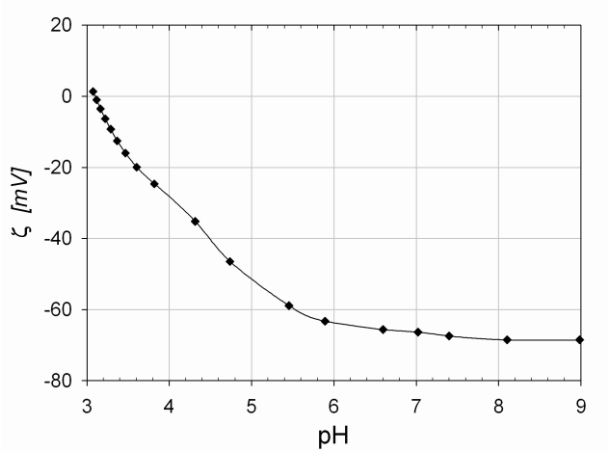

Figure 4. ζ potential in the presence of 10^{-3} M KCl as a function of pH for PMHS functionalized with 1,2-dilinoleoyl-sn-glycero-3-phosphorylcholine (18:2 Cis)

To summarize, all SiH groups have reacted. The reaction of PL with silane was not complete due to the bulkiness of the phospholipid chains, on the one hand, and competitive reaction with water from air moisture, catalyzed by Karstedt's catalyst, on the other hand. In the 5-10 nm upper layer the SiH reaction yield with double bonds (*ca* 45%) was higher than in the bulk (mean value *ca.* 15% as obtained from transmission infrared absorption), showing the preferential reaction of PL at the top of the PMHS layer.

Physical characterization of PMHS and PL-PMHS films

The final PL-PMHS film was characterized by AFM and SEM microscopy (Figs. 5,6). The pristine PMHS was very flat with low AFM roughness of 0.4 nm typical of sol-gel PMHS thin-film preparation. [53] After hydrosilylation, the major change of the surface topography by comparison with the virgin PMHS was the formation of grooves *ca.*100 nm deep which represented less than 10% of the total film thickness. Both reactions of the surface SiH functional groups in pristine PMHS with water and the

double bonds of the phospholipids PL increased the degree of crosslinking of the polymer chain in the PMHS network. The increasing crosslinking of the material may influence the thickness and surface roughness of the film as a consequence of the ensuing constraint. From cross sectional SEM images of the film, we observed, however, that the top of the PL-PMHS material was relatively flat showing that there were no grooves descending to the silicon substrate and no delamination of the film. Surface analysis by SEM showed a skin-like topography with the same peculiarities as in the AFM pictures over some larger areas and without defects. This result confirmed the good coverage of the PL-PMHS layer on the silicon substrate and the presence of superficial grooves. The surface morphological images under dry and aqueous conditions were studied using AFM (not shown). Some influence of water was detected as the depth of the grooves increased by about 20%.

Fig. 5 shows the cross-sectional SEM images of PMHS and PL-PMHS. The thickness after reaction was 170% higher than before grafting. The swelling can be attributed to the reaction with water and phospholipids. Swelling has also been observed by ellipsometry for n-alkene grafting reactions in PMHS siloxane networks.[55]

The water-wettability of the PL-PMHS surface was considerably greater than that of the untreated PMHS surface (Fig. 5). We preferred to examine hydrophilicity by the captive air bubble method as the material changed its interfacial character in response to the type of environment, air or aqueous medium. Indeed, the phosphorylcholine head at the surface can reorient slowly in a few hours as shown by the contact angle of a sessile drop of water which decreased from about 75° after droplet deposition to less than 5° after 1h under *RH* 80% humidity before evaporation of the droplet (not shown). This change was drastic with respect to PMHS characterized by an angle of 106°. By dipping the sample in water the captive air bubble angle increased with time from 130-150° after a few minutes, to 180° after several hours. At equilibrium (typically 15h), at room temperature, the air bubble could not adhere to the surface with contact angles of *ca.* 180°. We could explain this behaviour by the embedding of the hydrophilic phosphorylcholine head under the surface when the material was kept in contact with air while the reverse process occurred in the presence of water.[67, 68] In this case the phosphorylcholine heads migrated

to the uppermost surface. The water could also be trapped in the specific microstructured grooves leading to a superhydrophilic effect.

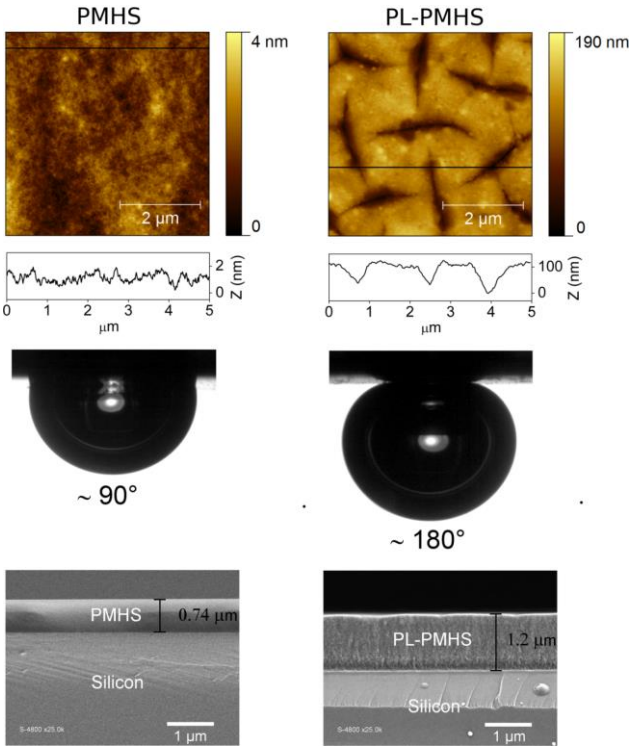

Figure 5 Surface analysis of PMHS (left) and PL-PMHS (right). From top to bottom: AFM images (5 × 5 μm^2) by tapping mode in air with corresponding *Z*-profile (black line) - PMHS with 0.4 nm roughness R_q and PL-PMHS with 100 nm deep grooves -. Captive air bubble contact angle in water. Cross-section images (Scanning Electronic Microscopy).

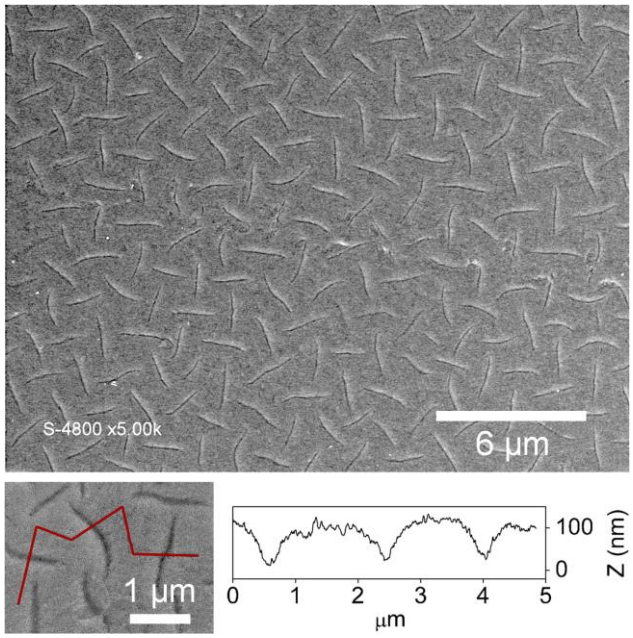

Figure 6 (top) SEM images of PL-PMHS over 25 × 20 µm^2 showing the same peculiarities as the AFM pictures. (bottom) Magnified 3D-SEM image with the corresponding *Z*-profile (broken line).

Adsorption of proteins

We examined the behavior of different proteins: avidin, bovine serum albumin (BSA), bovine fibrinogen, lysozyme and α-chymotrypsin. Given their isoelectric point, at physiological pH 7.4 BSA (67 000 g mol^{-1}, pI 5.6) is negative as fibrinogen (340 000 g mol^{-1}, pI 5.5), α-chymotrypsin (25 300 g mol^{-1}, pI 8.1) is slightly positive, avidin (66 000g mol^{-1}, pI 10) and lysozyme (14 300, pI 11) are strongly positive. Avidin is a model of a very stable hard protein. Conversely BSA, like fibrinogen, can be viewed as a model of a soft protein, able to be adsorbed and denatured on many materials whatever their charge. In addition, avidin is positive at neutral pH, thereby providing an electrostatic attractive component of interaction with negative substrates such as oxidized silicon wafers and glass. Avidin and BSA have about the same molecular mass. The two smaller other proteins should present a strong (lysozyme) or weak (α-chymotrypsin) electrostatic attractive component with a negative surface.

In Fig. 7 the adsorption kinetics of avidin from 10.5 µg / mL (150 nM) solutions in phosphate buffer 10 mM, 150 mM NaCl on the three surfaces, hydrophilic glass, 1µm thick PMHS coating, and a layer of PMHS functionalized with 1,2-dilinoleoyl-sn-glycero-3-phosphorylcholine (18:2 Cis) are depicted.

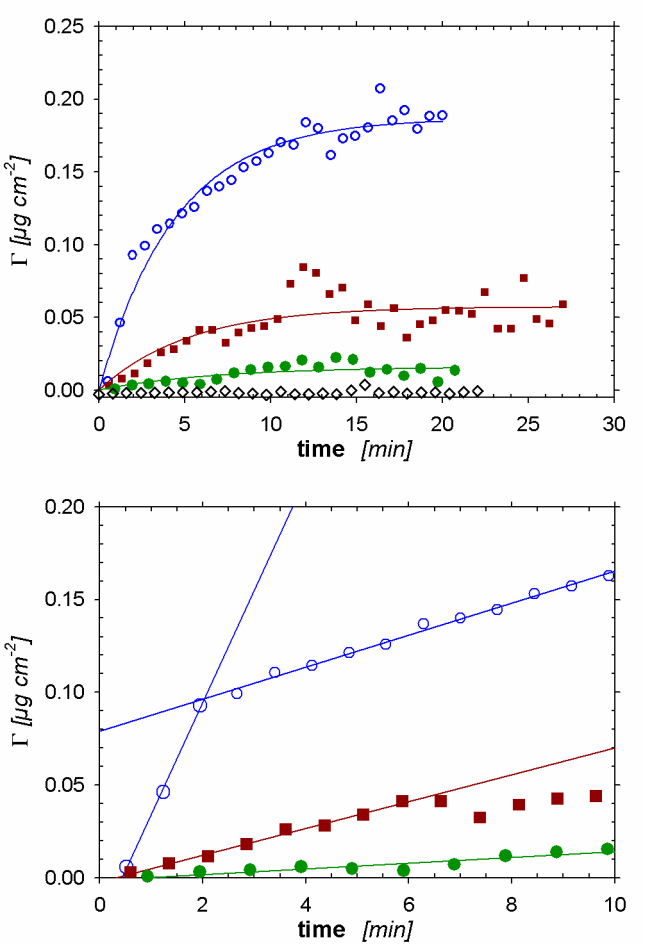

Figure 7. (top) Adsorption kinetics of avidin (10.5 µg /mL) in phosphate buffer saline at pH 7.4 on (o) sulfochromic treated glass, (■) polymethylhydrosiloxane (PMHS), (•) PMHS functionalized with 1,2-dilinoleoyl-sn-glycero-3-phosphorylcholine (18:2 Cis) immediately after reaction and (◊) after conditioning the interface overnight in buffer. Lines added as guide to the eye. (bottom) Initial kinetics fitted by linear functions to estimate the constant $k = (1/C_b)\,(d\Gamma/dt)_{t=0} \pm$ Std Err. (o) hydrophilic glass; $k = (0.96 \pm 0.04) \times 10^{-4}$ cm/s; (■) PMHS, $k = (1.15 \pm 0.05) \times 10^{-5}$ cm/s; (•) PL-PMHS, $k = (2.4 \pm 0.4) \times 10^{-6}$ cm/s.

In the neutral pH range, avidin is largely positive, as its isoelectric point is 10.4, and was expected to have an electrostatic attraction component with the negative hydrophilic glass, despite the quite high ionic strength. Indeed, we observed such adsorption. In the presence of the PMHS layer, adsorption still occurred but was significantly reduced. Finally, the treatment of PMHS with 1,2-dilinoleoyl-sn-glycero-3-phosphorylcholine (18:2 Cis) reduced still further the interfacial concentration of avidin. However, as we could expect some conformational changes in the PL-PMHS layer depending on the fluid at the interface, air or aqueous medium, the adsorption kinetics of avidin were studied after keeping the cell in buffer for different times: 0; 3 and 15 hours. Some tiny adsorption was still detectable after 3 hours but no adsorption at all after 15 hours (Fig. 10). The decreasing adsorption level observed after the successive treatments may be linked to the expected decreasing density of negative charges. The final totally repellent character of PL-PMHS was interpreted as resulting from the highly hydrated layer generated by the phosphorylcholine groups.

The initial kinetics were analyzed to estimate the adsorption constants. On hydrophilic glass, a two-step process can be proposed with an initial fast adsorption of constant $k \approx 10^{-4}$ cm s^{-1} of the same order of magnitude as the transport-controlled Lévêque model constant $k_{Lev} = 0.54\ (D^2\gamma/x)^{1/3} = 2.9 \times 10^{-4}$ cm s^{-1} with $D \approx 7 \times 10^{-7}$ cm^2 s^{-1}, $\gamma = 1000$ s^{-1} and x = 3 cm. The chemical constant k_a was therefore of the same order of magnitude. Applying previously published accurate approximations[69, 70] ($k_a = k\ (b_1\ u + 1)\ (b_2\ u + 1)/((u\text{-}1)\ (a_1\ u\text{-}1))$ where $u = k/k_{Lev}$ and numerical coefficients $a_1 = 0.556$, $b_1 = -0.681$, $b_2 = -0.0484$) led indeed to $k_a = 1.3 \times 10^{-4}$ cm s^{-1}. For the other interfaces, the constants were much smaller. The transport contribution was thus small and the k values were very close to the constant relative to the chemical control of the process: $k_a = 1.2 \times 10^{-5}$ cm/s and 2.4×10^{-6} cm/s for PMHS and PL-PMHS interfaces, respectively. The low adsorption level on PMHS seems not to be related to the hydrophobic character of the material. This behavior might be connected to the hard nature of avidin which prevents the protein to be denatured and expose its hydrophobic core to the PMHS surface.

The protein-repellent character of the PL-PMHS surface previously immersed overnight in water was also checked in the configuration of flowing solutions of α-chymotrypsin, lysozyme, BSA and fibrinogen (Fig. 8). Lysozyme is a hard protein positively charged like avidin at neutral pH. Conversely the negative BSA can be viewed as a model of soft protein, able to be adsorbed and denatured on many materials whatever their charge, thus a good candidate to check the possible hydrophobic interactions with surfaces. Indeed, this protein is often used in blocking buffers to prevent subsequent non specific adsorption[2]. BSA at 10, 50 and 100 µg/mL exhibited a final adsorption of 0.05, 0.2 and 0.3 ng cm^{-2} respectively, after relative significant desorption at the highest solution concentrations from about 1 and 2 ng cm^{-2} . Let us mention that there was a slight displacement in the plane of substrate between the normal scannings to avoid repetitive expositions to the laser beam which could induce a photobleaching effect. This procedure constituted then also an examination of the interface homogeneity. The repellent character of the PL-PMHS interface with respect to bovine serum albumin suggested that the phospholipid fatty chains were not able to protrude towards the protein for hydrophobic interactions.

The other proteins exhibited also low adsorption (Γ± SD). α-chymotrypsin: 0.15 ± 0.05; 0.50 ± 0.16; 0.73 ± 0.14 ng cm^{-2} ; Lyosozme: 0.08 ± 0.07; 0.3 ± 0.3; 0.46 ± 0.11 ng cm^{-2} ; Fibrinogen: 0.5 ± 0.3; 0.3 ± 0.1; 7 ± 2 ng cm^{-2}, from solutions at 10, 50 and 100 µg/mL respectively. The relatively high adsorption from the fibrinogen solution at 100 µg/mL might correspond to a domain with some surface defect.

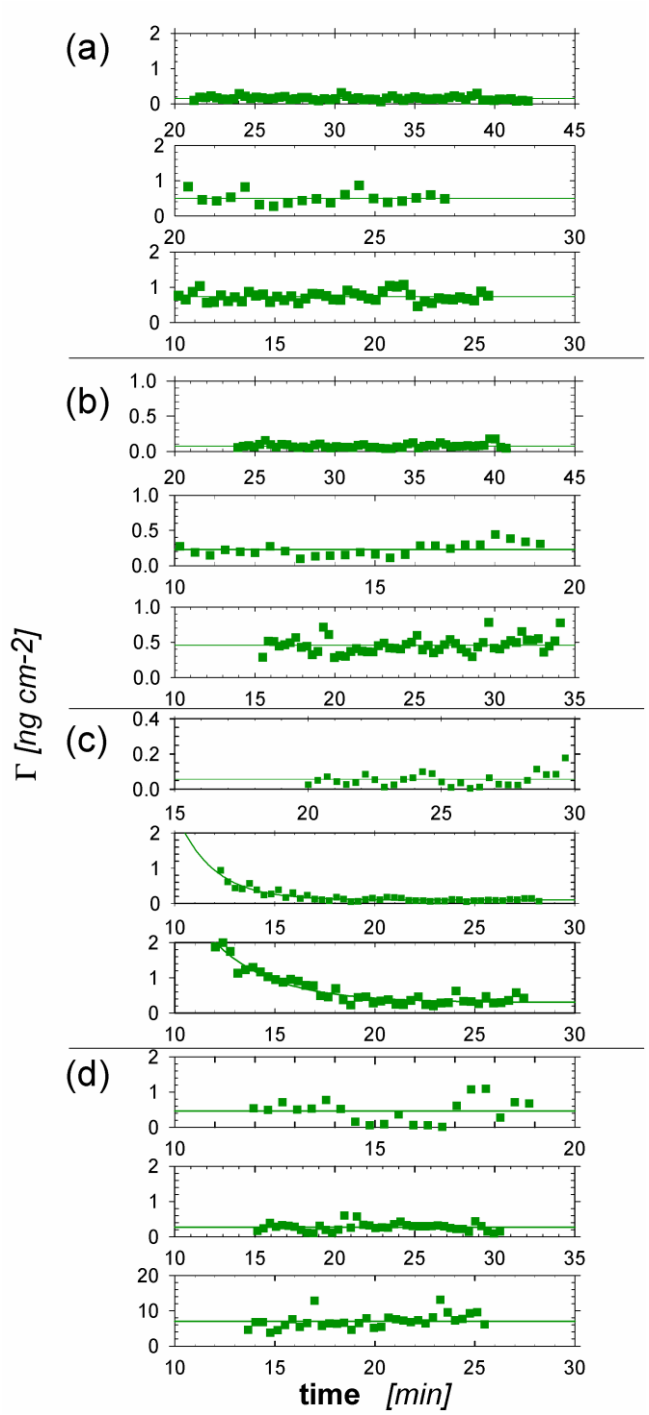

Figure 8 Interfacial concentration of proteins on PL-PMHS interface in the presence of flowing PBS buffer after flowing solutions at wall shear rate 1000 s^{-1}. C_b = 10; 50; 100 µg/mL (top to bottom). (a) α-chymotrypsin; (b) Lysozyme; (c) BSA; (d) Bovine Fibrinogen. T = 20°C.

Further functionalization

Infrared and XPS analysis after PMHS hydrosilylation with PL indicated the side reaction with water giving silanol groups, which may also evolve to siloxane crosslinks. In that case, such interfacial groups could be available for subsequent reaction. The presence of interfacial SiOH groups was checked by reaction of a monoethoxy silane coupling agent bearing alexa as fluorescent probe (Scheme 1). We indeed observed a high fluorescence signal thus confirming the possibilities of chemical functionalization at such a surface having an inert background of C18-phospholipids bearing a phosphorylcholine head. No coupling reaction occurred after pretreatment of PL-PMHS with hexamethyldisilazane (HMDS) as the silanols were neutralized by the bulky trimethylsilyl groups.

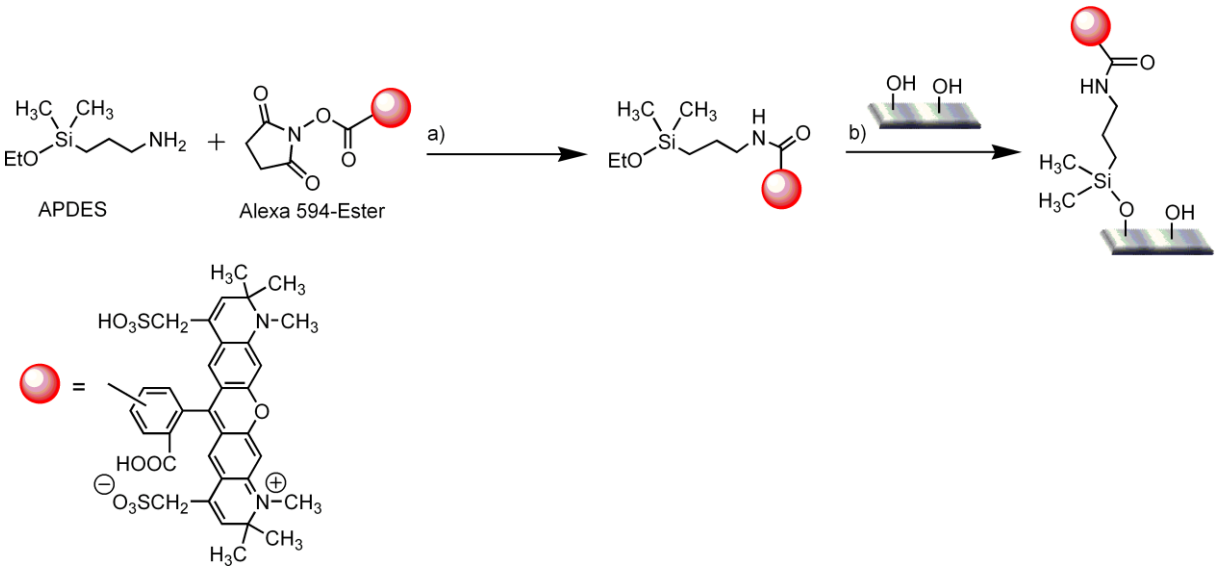

Scheme 1 Grafting reaction (b) of Alexa to surface silanols *via* (a) previous formation of amide links between alexa and the monoethoxy silane coupling agent.

PMHS did not exhibit any coupling reaction with alexa monoethoxy silane in toluene / ethanol (70/30), thus suggesting the relative stability of the interfacial hydrogenosilane (SiH) functional groups in the absence of water. Moreover, this demonstrates that the Karstedt'catatyzed side reaction of SiH with water plays a major role in the formation of interfacial silanol on the PL-PMHS surface. After coupling the alexa probe, the silanol concentration can be thus estimated by assuming that the coupling reaction is total. According to the method developed above for determination of interfacial concentration, which

may be an alternative to the removal of the fluorescent probe from surface to solution for analysis, [71] the mean degree of functionalization of the PL-PMHS layer was found to be 3.0×10^{-2} nm^{-2}. Assuming that all molecules were grafted at the interface the mean distance between the sites was 5.7 nm. This order of magnitude is acceptable for a quite dense packing of bigger molecules on a neutral background and can be probably modulated by experimental conditions. The interfacial crosslinking density might also be decreased by using phospholipids with fewer unsaturated carbon-carbon bonds which would lead to interfaces of different softness. However a better control of the side reaction with water would be needed.

Conclusion

Polymethylhydrosiloxane anchored on an oxidized silicon wafer or activated glass could be functionalized with phosphorylcholine heads by means of 1,2-dilinoleoyl-sn-glycero-3-phosphorylcholine (18:2 Cis). The functionality of the surface was checked by infrared absorbance and the correlated wettability change measured via contact angle measurements, with water drop or captive air bubble. Infrared absorption analysis demonstrated that all four double bonds of the phospholipids reacted with silane groups. XPS analysis showed a higher PL functionality at the interface than in the bulk. Side reaction with water provided the formation of silanol groups inducing probable swelling of the film and further possibilities of functionalization at the interface. The latter point was illustrated by grafting a fluorescent monoethoxy silane. Extension to the creation of amino functionalized interfaces should present no specific difficulties. The new interface was observed to be repellent towards avidin, bovine serum albumin, fibrinogen, lysozyme and α-chymotrypsin adsorption at neutral pH in phosphate saline buffer. Therefore, this work opens the way to the constitution of stable protein repellent interfaces which could be useful in several fields such as biomaterials, diagnostic kits, microfluidics and cell cultures. Compared to phospholipid polymerization[26] at 70°C, the present method avoided the tedious

preliminary preparation of the specific phospholipid with the needed polymerizable group in the fatty chains. In addition, in the present work, the reaction still occurred at room temperature and the final layer was anchored at the surface with a very hydrophilic character measured by captive air bubble contact angle. Such preliminary chemistry was also required for monolayer anchoring of phospholipids on surfaces[27]. With respect to those works and others[40] involving monolayers at interfaces, the present method was much simpler and could be extended easily to other phospholipids. Moreover, the initial PMHS layer provided a much higher density of reaction sites compared to other similar materials[54] thus providing its very hydrophilic character.

Given the different possibilities of varying the preparation conditions and in view of the perspectives, possible control of the structure, density and depth of the grooves, and softness of the interface could be achieved, both properties potentially useful in cell culture and tissue engineering. If, however, very flat surfaces are desired for AFM analysis, for instance, the regular network of 100 nm deep grooves should be avoided in principle.

Acknowledgments This work was supported by FP7 European grant NMP-214538 (BISNES project) and French Carnot structure. We are grateful to M. Ramonda (LMCP, UM2) for the AFM pictures, to Didier Cot (IEM) for the SEM pictures. Special thanks to Anton-Paar company for giving access to the SurPass apparatus for ζ potential measurements and to M. Leman for assistance in its use. JMJ is grateful to PI-France for discussions about the components of the optical device.

References

1. Lee, J.; Icoz, K.; Roberts, A.; Ellington, A. D.; Savran, C. A., *Anal. Chem.* **2010,** 82, 197-202.
2. Holmberg, M.; Hou, X. L., *Colloids and Surfaces B-Biointerfaces* **2011,** 84, 71-75.
3. Yan, F.; Dejardin, P.; Mulvihill, J. N.; Cazenave, J. P.; Crost, T.; Thomas, M.; Pusineri, C., *Journal of Biomaterials Science-Polymer Edition* **1992,** 3, 389-402.
4. Vermette, P.; Meagher, L., *Colloids and Surfaces B-Biointerfaces* **2003,** 28, 153-198.
5. Lee, J.; Kopecek, J.; Andrade, J., *Journal of Biomedical Materials Research* **1989,** 23, 351-368.

6. Wu, Y. J.; Timmons, R. B.; Jen, J. S.; Molock, F. E., *Colloids and Surfaces B: Biointerfaces* **2000,** 18, 235-248.
7. Maste, M. C. L.; van Velthoven, A. P. C. M.; Norde, W.; Lyklema, J., *Colloids and Surfaces A: Physicochemical and Engineering Aspects* **1994,** 83, 255-260.
8. Archambault, J. G.; Brash, J. L., *Colloids and Surfaces B-Biointerfaces* **2004,** 39, 9-16.
9. Du, Y. J.; Brash, J. L., *J. Appl. Polym. Sci.* **2003,** 90, 594-607.
10. Cecchet, F.; De Meersman, B.; Demoustier-Champagne, S.; Nysten, B.; Jonas, A. M., *Langmuir* **2006,** 22, 1173-1181.
11. Unsworth, L. D.; Sheardown, H.; Brash, J. L., *Langmuir* **2008,** 24, 1924-1929.
12. Tan, J.; McClung, W. G.; Brash, J. L., *Journal of Biomedical Materials Research Part A* **2008,** 85A, 873-880.
13. Tan, J.; Brash, J. L., *J. Appl. Polym. Sci.* **2008,** 108, 1617-1628.
14. Holmberg, M.; Hou, X. L., *Langmuir* **2010,** 26, 938-942.
15. Ionov, L.; Synytska, A.; Kaul, E.; Diez, S., *Biomacromolecules* **2010,** 11, 233-237.
16. Trmcic-Cvitas, J.; Hasan, E.; Ramstedt, M.; Li, X.; Cooper, M. A.; Abell, C.; Huck, W. T. S.; Gautrot, J. E., *Biomacromolecules* **2009,** 10, 2885-2894.
17. Su, Y. L.; Li, C., *React. Funct. Polym.* **2008,** 68, 161-168.
18. Yang, W.; Xue, H.; Li, W.; Zhang, J. L.; Jiang, S. Y., *Langmuir* **2009,** 25, 11911-11916.
19. Liu, P. S.; Chen, Q.; Liu, X.; Yuan, B.; Wu, S. S.; Shen, J.; Lin, S. C., *Biomacromolecules* **2009,** 10, 2809-2816.
20. Zwaal, R., *Nature* **1977,** 268, 358.
21. Chapman, D., *Langmuir* **1993,** 9, 39-45.
22. Hall, B.; Bird, R. L.; Chapman, D., *Angew. Makromol. Chem.* **1989,** 166, 169-178.
23. Leaver, J.; Alonso, A.; Durrani, A. A.; Chapman, D., *Biochim. Biophys. Acta* **1983,** 732, 210-218.
24. Albrecht, O.; Johnston, D. S.; Villaverde, C.; Chapman, D., *Biochim. Biophys. Acta* **1982,** 687, 165-169.
25. Johnston, D. S.; Sanghera, S.; Pons, M.; Chapman, D., *Biochim. Biophys. Acta* **1980,** 602, 57-69.
26. Marra, K. G.; Winger, T. M.; Hanson, S. R.; Chaikof, E. L., *Macromolecules* **1997,** 30, 6483-6488.
27. Kohler, A. S.; Parks, P. J.; Mooradian, D. L.; Rao, G. H. R.; Furcht, L. T., *Journal of Biomedical Materials Research* **1996,** 32, 237-242.
28. Ishihara, K.; Ziats, N. P.; Tierney, B. P.; Nakabayashi, N.; Anderson, J. M., *Journal of Biomedical Materials Research* **1991,** 25, 1397-1407.
29. Ishihara, K.; Takayama, R.; Nakabayashi, N.; Fukumoto, K.; Aoki, J., *Biomaterials* **1992,** 13, 235-239.
30. Furuzono, T.; Ishihara, K.; Nakabayashi, N.; Tamada, Y., *Biomaterials* **2000,** 21, 327-333.
31. Konno, T.; Kurita, K.; Iwasaki, Y.; Nakabayashi, N.; Ishihara, K., *Biomaterials* **2001,** 22, 1883-1889.
32. Jang, K.; Sato, K.; Mawatari, K.; Konno, T.; Ishihara, K.; Kitamori, T., *Biomaterials* **2009,** 30, 1413-1420.
33. Xu, Y.; Takai, M.; Ishihara, K., *Biomacromolecules* **2009,** 10, 267-274.
34. Goda, T.; Konno, T.; Takai, M.; Moro, T.; Ishihara, K., *Biomaterials* **2006,** 27, 5151-5160.
35. Chen, M.; Briscoe, W. H.; Armes, S. P.; Klein, J., *Science* **2009,** 323, 1698-1701.
36. Cheng, G.; Li, G. Z.; Xue, H.; Chen, S. F.; Bryers, J. D.; Jiang, S. Y., *Biomaterials* **2009,** 30, 5234-5240.
37. Feng, W.; Brash, J. L.; Zhu, S. P., *Biomaterials* **2006,** 27, 847-855.
38. Ye, S. H.; Johnson, C. A.; Woolley, J. R.; Murata, H.; Gamble, L. J.; Ishihara, K.; Wagner, W. R., *Colloids and Surfaces B-Biointerfaces* **2010,** 79, 357-364.
39. Reisch, A.; Voegel, J. C.; Decher, G.; Schaaf, P.; Mesini, P. J., *Macromolecular Rapid Communications* **2007,** 28, 2217-2223.

40. Tegoulia, V. A.; Cooper, S. L., *Journal of Biomedical Materials Research* **2000,** 50, 291-301.
41. Dormidontova, E. E., *Macromolecules* **2002,** 35, 987-1001.
42. Ostuni, E.; Chapman, R. G.; Holmlin, R. E.; Takayama, S.; Whitesides, G. M., *Langmuir* **2001,** 17, 5605-5620.
43. Olander, B.; Wirsen, A.; Albertsson, A. C., *Biomacromolecules* **2002,** 3, 505-510.
44. Chen, H.; Brook, M. A.; Sheardown, H. D.; Chen, Y.; Klenkler, B., *Bioconjugate Chemistry* **2006,** 17, 21-28.
45. Chen, H.; Zhang, Z.; Chen, Y.; Brook, M. A.; Sheardown, H., *Biomaterials* **2005,** 26, 2391-2399.
46. Chen, H.; Brook, M. A.; Sheardown, H., *Biomaterials* **2004,** 25, 2273-2282.
47. Thompson, D. B.; Fawcett, A. S.; Brook, M. A., *Silicon Based Polymers: Advances in Synthesis and Supramolecular Organization* **2008**, 29-38.
48. Guo, D. J.; Han, H. M.; Jing, W.; Xiao, S. J.; Dai, Z. D., *Colloids and Surfaces A-Physicochemical and Engineering Aspects* **2007,** 308, 129-135.
49. Speier, J. L., *Adv. Organomet. Chem.* **1979,** 17, 407-447.
50. Lewis, L. N., *Chemical Reviews* **1993,** 93, 2693-2730.
51. Brook, M. A., *Biomaterials* **2006,** 27, 3274-3286.
52. Yactine, B.; Ganachaud, F.; Senhaji, O.; Boutevin, B., *Macromolecules* **2005,** 38, 2230-2236.
53. Thami, T.; Bresson, B.; Fretigny, C., *J. Appl. Polym. Sci.* **2007,** 104, 1504-1516.
54. Ishihara, K.; Ando, B.; Takai, M., *Nanobiotechnology* **2007,** 3, 83-88.
55. Thami, T.; Nasr, G.; Bestal, H.; van der Lee, A.; Bresson, B., *Journal of Polymer Science Part a-Polymer Chemistry* **2008,** 46, 3546-3562.
56. Nasr, G.; Bestal, H.; Barboiu, M.; Bresson, B.; Thami, T., *J. Appl. Polym. Sci.* **2009,** 111, 2785-2797.
57. Stine, R.; Pishko, M. V.; Hampton, J. R.; Dameron, A. A.; Weiss, P. S., *Langmuir* **2005,** 21, 11352-11356.
58. Ross, E. E.; Rozanski, L. J.; Spratt, T.; Liu, S. C.; O'Brien, D. F.; Saavedra, S. S., *Langmuir* **2003,** 19, 1752-1765.
59. Ross, E. E.; Spratt, T.; Liu, S. C.; Rozanski, L. J.; O'Brien, D. F.; Saavedra, S. S., *Langmuir* **2003,** 19, 1766-1774.
60. Amro, K.; Clement, S.; Dejardin, P.; Douglas, W. E.; Gerbier, P.; Janot, J. M.; Thami, T., *J. Mater. Chem.* **2010,** 20, 7100-7103.
61. Balme, S.; Janot, J.-M.; Dejardin, P.; Seta, P., *Journal of Photochemistry and Photobiology A: Chemistry* **2006,** 184, 204-211.
62. Melamed, M. D.; Green, N. M., *Biochem. J.* **1963,** 89, 591-&.
63. Scofield, J. H., *J. Electron Spectrosc. Relat. Phenom.* **1976,** 8, 129-137.
64. Beamson, G.; Briggs, D., *High resolution XPS of organic polymers*. Wiley: Chichester, 1992.
65. Balme, S.; Janot, J.-M.; Dejardin, P.; Vasina, E. N.; Seta, P., *J. Membr. Sci.* **2006,** 284, 198-204.
66. Janot, J.-M.; Boissiere, M.; Thami, T.; Tronel-Peyroz, E.; Helassa, N.; Noinville, S.; Quiquampoix, H.; Staunton, S.; Dejardin, P., *Biomacromolecules* **2010,** 11, 1661-1666.
67. Futamura, K.; Matsuno, R.; Konno, T.; Takai, M.; Ishihara, K., *Langmuir* **2008,** 24, 10340-10344.
68. Yang, S.; Zhang, S. P.; Winnik, F. M.; Mwale, F.; Gong, Y. K., *Journal of Biomedical Materials Research Part A* **2008,** 84A, 837-841.
69. Noinville, S.; Vidic, J.; Dejardin, P., *Colloids and Surfaces B-Biointerfaces* **2010,** 76, 112-116.
70. Dejardin, P.; Vasina, E. N., *Colloids and Surfaces B: Biointerfaces* **2004,** 33, 121-127.
71. Tauk, L.; Schroder, A. P.; Decher, G.; Giuseppone, N., *Nat. Chem.* **2009,** 1, 649-656.

TOC Graphic